Title
Zirconium oxide surface passivation of crystalline silicon

Journal
Applied Physics Letters, 112(20)

ISSN
0003-6951

Authors
Wan, Yimao
Bullock, James
Hettick, Mark
et al.

Publication Date
2018-05-14

DOI
10.1063/1.5032226

Peer reviewed

Zirconium oxide surface passivation of crystalline silicon

Appl. Phys. Lett. **112**, 201604 (2018); https://doi.org/10.1063/1.5032226

Yimao Wan[1,2,3,a)], James Bullock[2,3], Mark Hettick[2,3], Zhaoran Xu[2,3], Di Yan[1], Jun Peng[1], Ali Javey[2,3], *and* Andres Cuevas[1]
View Affiliations

ABSTRACT

This letter reports effective passivation of crystalline silicon (c-Si) surfaces by thermal atomic layer deposited zirconium oxide (ZrO_x). The optimum layer thickness and activation annealing conditions are determined to be 20 nm and 300 °C for 20 min. Cross-sectional transmission electron microscopy imaging shows an approximately 1.6 nm thick SiO_x interfacial layer underneath an 18 nm ZrO_x layer, consistent with ellipsometry measurements (∼20 nm). Capacitance–voltage measurements show that the annealed ZrO_x film features a low interface defect density of 1.0×10^{11} $cm^{-2}eV^{-1}$ and a low negative film charge density of -6×10^{10} cm^{-2}. Effective lifetimes of 673 μs and 1.1 ms are achieved on *p*-type and *n*-type 1 Ω cm undiffused c-Si wafers, respectively, corresponding to an implied open circuit voltage above 720 mV in both cases. The results demonstrate that surface passivation quality provided by ALD ZrO_x is consistent with the requirements of high efficiency silicon solar cells.

Crystalline silicon (c-Si) solar cells remain the most successful photovoltaic technology due to a combination of high power conversion efficiency and

low manufacturing cost. One of the key enablers in achieving high performance has been the passivation of the dangling bonds usually present on the silicon wafer surfaces. The most extensively explored, and implemented in industry, materials to suppress defect-assisted Shockley-Read-Hall (SRH) recombination are thermally grown or plasma deposited thin films of silicon oxide (SiO_2),[1] silicon nitride (SiN_x),[2,3] amorphous silicon (a-Si),[4] and aluminium oxide (Al_2O_3).[5,6] Recently, a range of transition or post-transition metal oxides have also been demonstrated to provide high quality passivation of silicon surfaces, including titanium oxide,[7,8] hafnium oxide,[9–12] gallium oxide,[13] and tantalum oxide.[14,15]

Zirconium oxide (ZrO_x) is another transition metal oxide having high potential to be compatible with photovoltaic applications, as it has reasonable optical properties (i.e., a relatively high refractive index and a negligible absorption in the visible range) to be used as antireflection coating.[16] It has also been reported to provide some passivation of titanium oxide surfaces.[17] In the semiconductor industry, ZrO_x has been extensively investigated as an alternative to SiO_2 as a gate insulator due to its high dielectric constant ($\sim$25), insulating properties, and relatively good thermal stability.[18–20] Indeed, binary alloy systems of ZrO_x/alumina or ZrO_x/yttria have been patented for the antireflection and passivation of silicon surfaces.[21,22] However, no scientific details have yet been published on such an ability of ZrO_x to suppress surface recombination in c-Si photovoltaic devices.

In this letter, we present evidence of effective surface passivation of c-Si by ZrO_x prepared by atomic layer deposition (ALD). The structure, composition,

and interfacial characteristics of this passivating layer are examined using cross-sectional transmission electron microscopy (TEM) and x-ray photoelectron spectroscopy (XPS). The passivation quality is then evaluated on undiffused *p*-type and *n*-type c-Si wafers. Furthermore, capacitance–voltage (C–V) measurements and X-ray diffraction (XRD) are undertaken to probe the electronic and crystal properties of ZrO_x films before and after thermal annealing to elucidate the physical mechanisms underlying the evolution in surface passivation.

The ZrO_x films were deposited in a thermal ALD system (Cambridge Savannah) using TEMAZ [Tetra(ethylmethylamido)zirconium] as the zirconium precursor, H_2O as the oxidant, and N_2 as the purge gas. The deposition was performed at 150 °C and had a corresponding rate of 1.33 Å/cycle as measured by *ex-situ* spectroscopic ellipsometry (J.A. Woollam M2000 ellipsometer) and also was confirmed by the high resolution TEM presented in Fig. 1(a). The cross section of the ZrO_x film was prepared using a focused ion beam (FIB) lift-out technique in a Helios NanoLab 600 DualBeam SEM/FIB system. Note that the film used for TEM is after thermal annealing (300 °C for 20 min in air), which is required to activate the passivation capability by ZrO_x. TEM images were taken using a JEOL ARM200F microscope operating at 200 kV. As shown in Fig. 1(a), there exists an approximately 1.6 nm thick interfacial layer and a ∼18 nm thick ZrO_x layer. The interfacial layer is typically observed for ALD deposited films[5,6] and likely resultant from exposure to water during the first few ALD cycles and/or possible reactions between ZrO_x and the c-Si surface.

Furthermore, the TEM also reveals that the ZrO_x film after annealing exhibits partial crystallization, which is validated by the XRD measurements presented in Fig. 1(b).

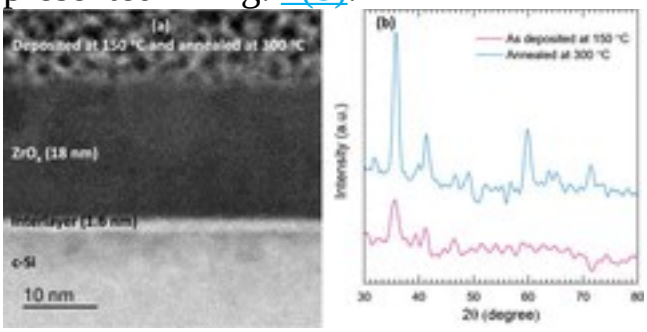

FIG. 1.(a) Cross-sectional TEM image showing an 18 nm ZrO_x film with an ~1.6 nm thick interfacial layer on c-Si and (b) XRD features of as-deposited and annealed ZrO_x films.

- PPT

|

- High-resolution

XRD measurements were performed on ZrO_x coated single-side polished c-Si wafers, using a PANalytical X'Pert PRO MRD diffractometer with an X-ray parabolic mirror and a parallel plate collimator (0.27°). The diffraction patterns were obtained by Ni-filtered Cu Ka radiation and analysed using the software package MDI Jade. Figure 1(b) plots the XRD pattern of ZrO_x films as deposited at 150 °C and annealed at 300 °C. As can be seen, the as-deposited film exhibits very weak diffraction features apart from a peak at 35°, indicating that the film may have some localised crystal nucleation, but is predominantly amorphous. In contrast, the film after thermal annealing

shows strong and distinctive diffraction features, consistent with the partial crystallization revealed by TEM in Fig. 1(a).

XPS measurements were performed to determine the stoichiometry of ALD ZrO_x films before and after annealing. Figure 2 shows the core levels of Zr 3d and O 1s. While the Zr 3d spectra show typical doublet peaks located at 182 eV and 184.5 eV for Zr $3d_{5/2}$ and Zr $3d_{3/2}$, respectively, the O 1s spectra can be fitted with two Gaussian components with peaks positioned at 530 eV and 531.5 eV, respectively.[23,24] The small peak located at 531.5 eV is usually attributed to hydroxyl groups although sometimes it can also be due to surface contamination. The component with lower binding energy peaked at 530 eV can be attributed to Zr–O binding. Notably, the peak positions for both Zr 3d and O 1s are observed to be the similar for the zirconia films before and after thermal annealing. The extracted zirconia film stoichiometry (i.e., O to Zr atomic fraction) based on core level peak areas is determined to be 2.0 and 1.8 for the film before and after annealing, respectively, implying that the thermal annealing process makes the film slightly sub-stoichiometric.

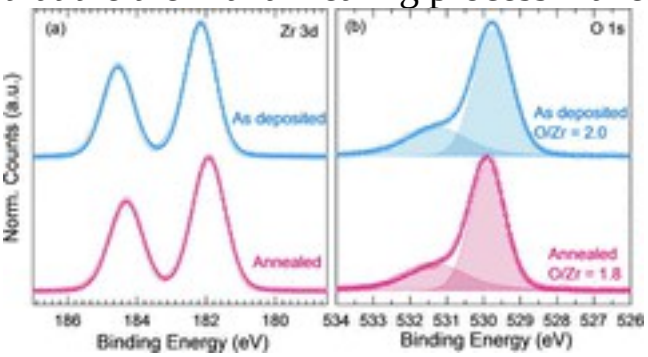

FIG. 2. The core level spectrum of (a) Zr 3d and (b) O 1s of as-deposited and annealed ZrO_x films measured by X-ray photoelectron spectroscopy (XPS) measurements.

- PPT

|

- High-resolution

To evaluate surface passivation of c-Si by the deposited dielectric, 1 Ω cm *n*-type and *p*-type c-Si substrates with a thickness of 200 μm were symmetrically coated with ALD ZrO_x films. All wafers were float-zone (FZ) grown and {100} oriented. The undiffused wafers were etched in tetramethylammonium hydroxide (TMAH, 25 wt. %) at ∼85 °C to remove saw damage. All samples were then cleaned by the RCA (Radio Corporation of America) procedure and dipped in 1% diluted HF acid to remove any remaining oxide prior to deposition. The effective carrier lifetime τ_{eff} as a function of excess carrier density Δn was measured using a Sinton Instruments WCT-120 photoconductance tool.[25] Neglecting Shockley–Read–Hall recombination in the bulk of the wafer, the upper limit of the effective surface recombination velocity $S_{eff,UL}$ was calculated according to $S_{eff,UL}=W2\left(\frac{1}{\tau_{eff}}-\frac{1}{\tau_{intrinsic}}\right)$, where W is the c-Si substrate thickness and $\tau_{intrinsic}$ is the intrinsic bulk lifetime of c-Si as parameterized by Richter *et al.*[26]

Figure 3 shows the measured effective lifetime provided by as-deposited and thermally activated ZrO_x films on *p*-type and *n*-type 1.0 Ω cm undiffused c-Si wafers. As can be seen, the as-deposited ZrO_x provides some surface passivation on both *p*-type and *n*-type wafers with a τ_{eff} value around 40 μs at $\Delta n = 10^{15}$ cm^{-3}. Upon thermal annealing at 300 °C for 20 min on a hotplate in

air, the level of surface passivation is vastly improved by more than one order of magnitude, resulting in τ_{eff} as high as 673 μs and 1.1 ms at $\Delta n = 10^{15}$ cm^{-3} on *p*-type and *n*-type c-Si, respectively. These lifetimes correspond to $S_{eff,UL}$ values of 13 cm/s and 8 cm/s and to implied open circuit voltages of 721 mV and 726 mV, respectively. The obtained $S_{eff,UL}$ by ZrO_x is slightly higher than that by conventional passivation layers such as SiN_x or Al_2O_3 and comparable to that by HfO_2, as summarized in Ref. 12.

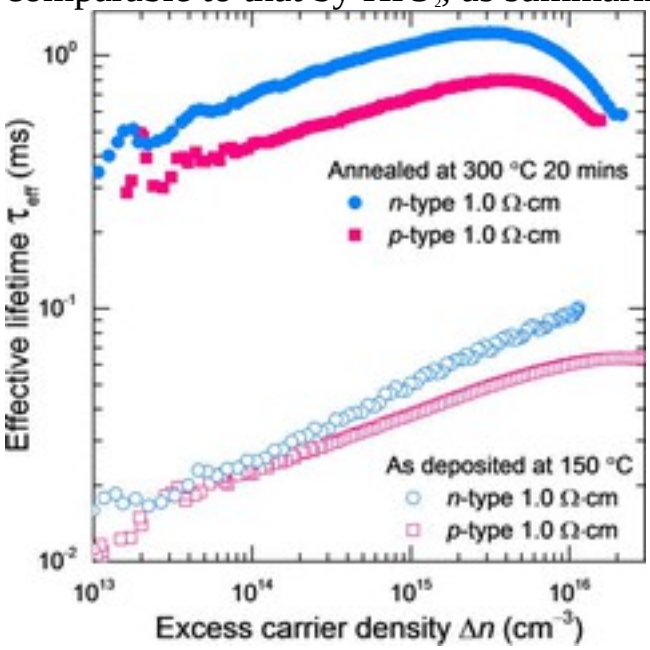

FIG. 3. Effective lifetime τ_{eff} as a function of excess carrier density Δn for *p*-type and *n*-type 1.0 Ω cm undiffused c-Si wafers passivated by as-deposited and annealed ZrO_x films.

- PPT

|

- High-resolution

C–V measurements were performed to evaluate the physical mechanisms for the substantial improvement in surface passivation upon thermal annealing, using a contactless corona charging method (Semilab PV2000A) on the same *n*-type and *p*-type c-Si samples used for the effective lifetime measurements.[27] The extracted interface defect density D_{it} and effective film charge density Q_{eff} are summarised in Table I. The results show that the as-deposited film presents a significant amount of defects at the ZrO_x/c-Si interface of 1.51×10^{12} $cm^{-2}eV^{-1}$, which is then drastically reduced by more than one order of magnitude to a level of 1.0×10^{11} $cm^{-2}eV^{-1}$ after annealing. The reduction in D_{it} is commonly ascribed to the hydrogenation of dangling bonds at the dielectric/c-Si interface, for example, for the case of passivation by SiN_x,[2,3] a-Si,[4] and Al_2O_3.[5,6] This could also be the case for ZrO_x passivation since the precursor is a hydrogen-containing organometallic compound. The effective charge density is at the order of 10^{10} cm^{-2} for both as-deposited and annealed samples, which is low compared to the charge density typically found in conventional silicon nitride or alumina films (i.e., $\sim 10^{12}$ cm^{-2}).[28,29] The thermal annealing switched the charge from positive 4.4×10^{10} cm^{-2} to negative 5.8×10^{10} cm^{-2}. The cause of the charge polarity change is still under investigation. Consistent results were obtained on both *n*-type and *p*-type substrates. Nevertheless, the substantial improvement in surface passivation by ZrO_x upon thermal annealing appears to be primarily attributable to a reduction in the interface defect density rather than to an increase in charge density since Q_{eff} is reasonably low.

TABLE I. Interface defect density D_{it} and effective fixed charge density Q_{eff} for ZrO_x films.

TABLE I. Interface defect density D_{it} and effective fixed charge density Q_{eff} for ZrO_x films.

	As-deposited *n*-type	**Annealed *n*-type**	**Annealed *p*-type**
$D_{it}(10^{11}cm^{-2}eV^{-1})$	15.1	1.0	1.2
$Q_{eff}/q(10^{10}cm^{-2})$	+4.4	−5.8	−5.9

The passivation quality by ZrO_x is shown in Fig. 4 to exhibit a strong dependence on film thickness, thermal annealing temperature, and time. As the film thickness increases, the effective lifetime first increases sharply and peaks at 20 nm. The passivation seems slightly less effective when ZrO_x becomes thicker. This thickness dependence is similar to that exhibited by ALD hafnium oxide presented by Cui *et al.*,[12] presumably due to higher crystallinity of thick films upon thermal annealing. A similar behaviour was observed for the dependence of thermal annealing temperature and time, showing an optimum condition at 300 °C for 20 min. It is worth mentioning that the degradation of passivation upon annealing above 300 °C could also be due to deterioration of silicon bulk quality, as presented in Ref. 30. As presented before, the thermal annealing activates the passivation by the ZrO_x film primarily through the reduction in interface defect density. The process window of annealing duration seems reasonably wide between 10

and 30 min. Note that the annealing was conducted on a hotplate in air. Our preliminary study of annealing in forming gas in the thermal furnace shows similar trends but slightly poorer passivation quality. The reason for this behaviour is still unknown to us and warrants further investigation.

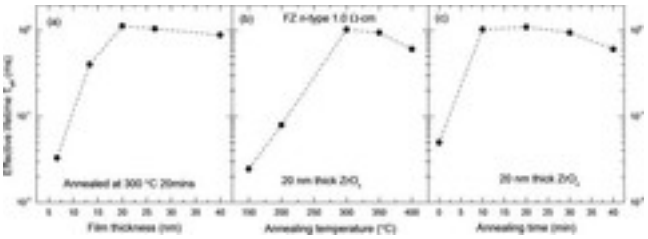

FIG. 4. The dependence of effective lifetime by ZrO_x passivation on (a) ZrO_x film thickness, (b) annealing temperature, and (c) annealing time.

- PPT

|

- High-resolution

In conclusion, we have shown effective surface passivation of c-Si wafers by thermal ALD ZrO_x with an optimum thickness at 20 nm and annealing at 300 °C for 20 min in air ambient. Effective lifetimes of 673 μs and 1.1 ms were achieved on *p*-type and *n*-type 1 Ω cm undiffused wafers, respectively, corresponding to $S_{eff,UL}$ values of 13 cm/s and 8 cm/s and an implied V_{OC} above 720 mV. C–V measurements revealed that the annealed ZrO_x film features a low D_{it} of 1.0×10^{11} $cm^{-2}eV^{-1}$ and a low negative Q_{eff} of -6×10^{10} cm^{-2}. The demonstrated high passivation by ALD ZrO_x paves the way for its application in the design and fabrication of high efficiency silicon solar cells.

We would like to thank Dr. Jason Cui for XRD measurements and analysis and Dr. Ziv Hameiri and Mr. Kyung Kim for contactless corona CV

measurements and analysis. This work was supported by the Australian Government through the Australian Research Council (Discovery Project No. DP150104331) and the Australia−U.S. Institute for Advanced Photovoltaics (AUSIAPV) program under Grant No. ACAP6.9. Y.W. holds Individual Fellowship from the Australian Center of Advanced Photovoltaics (ACAP). XPS characterization was performed at the Joint Center for Artificial Photosynthesis, supported through the Office of Science of the U.S. Department of Energy under Award No. DE-SC0004993. Material characterization was supported by the Electronic Materials Programs, funded by the Director, Office of Science, Office of Basic Energy Sciences, Material Sciences and Engineering Division of the U.S. Department of Energy under Contract No. DE-AC02-05CH11231.

REFERENCES

1. 1.M. J. Kerr and A. Cuevas, “Very low bulk and surface recombination in oxidized silicon wafers,” Semicond. Sci. Technol. **17**(1), 35 (2002). https://doi.org/10.1088/0268-1242/17/1/306, **Google ScholarCrossref**
2. 2.J. Schmidt and M. Kerr, “Highest-quality surface passivation of low-resistivity p-type silicon using stoichiometric PECVD silicon nitride,” Sol. Energy Mater. Sol. Cells **65**(1–4), 585 (2001). https://doi.org/10.1016/S0927-0248(00)00145-8, **Google ScholarCrossref**, CAS

3. 3.Y. Wan, K. R. McIntosh, A. F. Thomson, and A. Cuevas, “Low surface recombination velocity by low-absorption silicon nitride on c-Si,” IEEE J. Photovoltaics **3**(1), 554 (2013). https://doi.org/10.1109/JPHOTOV.2012.2215014, **Google ScholarCrossref**
4. 4.S. De Wolf and M. Kondo, “Abruptness of a-Si:H/c-Si interface revealed by carrier lifetime measurements,” Appl. Phys. Lett. **90**(4), 042111 (2007). https://doi.org/10.1063/1.2432297, **Google ScholarScitation**, **ISI**
5. 5.J. Schmidt, A. Merkle, R. Brendel, B. Hoex, M. C M. van de Sanden, and W. M. M. Kessels, “Surface passivation of high-efficiency silicon solar cells by atomic-layer-deposited Al_2O_3,” Prog. Photovoltaics: Res. Appl. **16**(6), 461 (2008). https://doi.org/10.1002/pip.823, **Google ScholarCrossref**, **CAS**
6. 6.B. Hoex, S. B. S. Heil, E. Langereis, M. C. M. van de Sanden, and W. M. M. Kessels, “Ultralow surface recombination of c-Si substrates passivated by plasma-assisted atomic layer deposited Al_2O_3,” Appl. Phys. Lett. **89**(4), 042112 (2006). https://doi.org/10.1063/1.2240736, **Google ScholarScitation**, **ISI**
7. 7.A. F. Thomson and K. R. McIntosh, “Light-enhanced surface passivation of TiO_2-coated silicon,” Prog. Photovoltaics: Res. Appl. **20**(3), 343 (2012). https://doi.org/10.1002/pip.1132, **Google ScholarCrossref**
8. 8.B. Liao, B. Hoex, A. G. Aberle, D. Chi, and C. S. Bhatia, “Excellent c-Si surface passivation by low-temperature atomic layer deposited titanium

oxide," Appl. Phys. Lett. **104**(25), 253903 (2014). https://doi.org/10.1063/1.4885096, **Google ScholarScitation**, **ISI**

9. 9.G. Dingemans and W. M. M. Kessels, "Aluminum oxide and other ALD materials for Si surface passivation," ECS Trans. **41**(2), 293 (2011). https://doi.org/10.1149/1.3633680, **Google ScholarCrossref**
10. 10.J. Wang, S. S. Mottaghian, and M. F. Baroughi, "Passivation properties of atomic-layer-deposited hafnium and aluminum oxides on Si surfaces," IEEE Trans. Electron Devices **59**(2), 342 (2012). https://doi.org/10.1109/TED.2011.2176943, **Google ScholarCrossref**
11. 11.F. Lin, B. Hoex, Y. H. Koh, J. J. Lin, and A. G. Aberle, "Low-temperature surface passivation of moderately doped crystalline silicon by atomic-layer-deposited hafnium oxide films," Energy Proc. **15**(0), 84 (2012). https://doi.org/10.1016/j.egypro.2012.02.010, **Google ScholarCrossref**
12. 12.J. Cui, Y. Wan, Y. Cui, Y. Chen, P. Verlinden, and A. Cuevas, "Highly effective electronic passivation of silicon surfaces by atomic layer deposited hafnium oxide," Appl. Phys. Lett. **110**(2), 021602 (2017). https://doi.org/10.1063/1.4973988, **Google ScholarScitation**, **ISI**
13. 13.T. G. Allen and A. Cuevas, "Electronic passivation of silicon surfaces by thin films of atomic layer deposited gallium oxide," Appl. Phys. Lett. **105**(3), 031601 (2014). https://doi.org/10.1063/1.4890737, **Google ScholarScitation**, **ISI**

14. 14.Y. Wan, J. Bullock, and A. Cuevas, “Passivation of c-Si surfaces by ALD tantalum oxide capped with PECVD silicon nitride,” Sol. Energy Mater. Sol. Cells **142**, 42 (2015). https://doi.org/10.1016/j.solmat.2015.05.032, **Google Scholar** **Crossref**

15. 15.Y. Wan, J. Bullock, and A. Cuevas, “Tantalum oxide/silicon nitride: A negatively charged surface passivation stack for silicon solar cells,” Appl. Phys. Lett. **106**(20), 201601 (2015). https://doi.org/10.1063/1.4921416, **Google Scholar** **Scitation**, **ISI**

16. 16.R. H. French, S. J. Glass, F. S. Ohuchi, Y. N. Xu, and W. Y. Ching, “Experimental and theoretical determination of the electronic structure and optical properties of three phases of ZrO_2,” Phys. Rev. B **49**(8), 5133 (1994). https://doi.org/10.1103/PhysRevB.49.5133, **Google Scholar** **Crossref**, **CAS**

17. 17.M. Vasilopoulou, D. G. Georgiadou, A. Soultati, N. Boukos, S. Gardelis, L. C. Palilis, M. Fakis, G. Skoulatakis, S. Kennou, M. Botzakaki, S. Georga, C. A. Krontiras, F. Auras, D. Fattakhova-Rohlfing, T. Bein, T. A. Papadopoulos, D. Davazoglou, and P. Argitis, “Atomic-layer-deposited aluminum and zirconium oxides for surface passivation of TiO_2 in high-efficiency organic photovoltaics,” Adv. Energy Mater. **4**(15), 1400214 (2014). https://doi.org/10.1002/aenm.201400214, **Google Scholar** **Crossref**

18. 18.A. Javey, H. Kim, M. Brink, Q. Wang, A. Ural, J. Guo, P. McIntyre, P. McEuen, M. Lundstrom, and H. Dai, “High-κ dielectrics for advanced

carbon-nanotube transistors and logic gates," Nat. Mater. **1**, 241 (2002). https://doi.org/10.1038/nmat769, **Google ScholarCrossref**, CAS

19. 19.C. M. Perkins, B. B. Triplett, P. C. McIntyre, K. C. Saraswat, S. Haukka, and M. Tuominen, "Electrical and materials properties of ZrO_2 gate dielectrics grown by atomic layer chemical vapor deposition," Appl. Phys. Lett. **78**(16), 2357 (2001). https://doi.org/10.1063/1.1362331, **Google ScholarScitation**, **ISI**, **CAS**

20. 20.C. M. Perkins, B. B. Triplett, P. C. McIntyre, K. C. Saraswat, and E. Shero, "Thermal stability of polycrystalline silicon electrodes on ZrO_2 gate dielectrics," Appl. Phys. Lett. **81**(8), 1417 (2002). https://doi.org/10.1063/1.1499513, **Google ScholarScitation**, **ISI**, **CAS**

21. 21.J. M. Hwang, Google patent US20120024336A1 (February 2, 2012). **Google Scholar**

22. 22.P. Pathi, R. Kalpana, S. K. Srivastava, C. M. S. Rauthan, and P. K. Singh, Google patent WO2017090059A1 (June 1, 2017). **Google Scholar**

23. 23.M. Cassir, F. Goubin, C. Bernay, P. Vernoux, and D. Lincot, "Synthesis of ZrO_2 thin films by atomic layer deposition: Growth kinetics, structural and electrical properties," Appl. Surf. Sci. **193**(1), 120 (2002). https://doi.org/10.1016/S0169-4332(02)00247-7, **Google ScholarCrossref**

24. 24.L. Sygellou, V. Gianneta, N. Xanthopoulos, D. Skarlatos, S. Georga, C. Krontiras, S. Ladas, and S. Kennou, "$ZrO_2$and Al_2O_3 thin films on Ge(100)

grown by ALD: An XPS investigation," Surf. Sci. Spectra **18**(1), 58 (2011). https://doi.org/10.1116/11.20100901, **Google ScholarCrossref**, CAS

25. 25.R. A. Sinton and A. Cuevas, "Contactless determination of current–voltage characteristics and minority-carrier lifetimes in semiconductors from quasi-steady-state photoconductance data," Appl. Phys. Lett. **69**(17), 2510 (1996). https://doi.org/10.1063/1.117723, **Google ScholarScitation**, **ISI**, **CAS**

26. 26.A. Richter, S. W. Glunz, F. Werner, J. Schmidt, and A. Cuevas, "Improved quantitative description of Auger recombination in crystalline silicon," Phys. Rev. B **86**(16), 165202 (2012). https://doi.org/10.1103/PhysRevB.86.165202, **Google ScholarCrossref**

27. 27.M. Wilson, J. D. Amico, A. Savtchouk, P. Edelman, A. Findlay, L. Jastrzebski, J. Lagowski, K. Kis-Szabo, F. Korsos, A. Toth, A. Pap, R. Kopecek, and K. Peter, paper presented at the 2011 37th IEEE Photovoltaic Specialists Conference, 2011. **Google Scholar**

28. 28.A. G. Aberle, "Overview on SiN surface passivation of crystalline silicon solar cells," Sol. Energy Mater Sol. Cells **65**(1–4), 239 (2001). https://doi.org/10.1016/S0927-0248(00)00099-4, **Google ScholarCrossref**, **CAS**

29. 29.L. E. Black and K. R. McIntosh, "Surface passivation of c-Si by atmospheric pressure chemical vapor deposition of Al_2O_3," Appl. Phys.

Lett. **100**(20), 202107 (2012). https://doi.org/10.1063/1.4718596, **Google ScholarScitation**, **ISI**

30. 30.N. E. Grant, V. P. Markevich, J. Mullins, A. R. Peaker, F. Rougieux, and D. Macdonald, “Thermal activation and deactivation of grown-in defects limiting the lifetime of float-zone silicon,” Phys. Status Solidi (RRL)–RRL **10**(6), 443 (2016). https://doi.org/10.1002/pssr.201600080, **Google ScholarCrossref**